Soft Matter

Accepted Manuscript

This is an *Accepted Manuscript*, which has been through the Royal Society of Chemistry peer review process and has been accepted for publication.

Accepted Manuscripts are published online shortly after acceptance, before technical editing, formatting and proof reading. Using this free service, authors can make their results available to the community, in citable form, before we publish the edited article. We will replace this *Accepted Manuscript* with the edited and formatted *Advance Article* as soon as it is available.

You can find more information about *Accepted Manuscripts* in the Information for Authors.

Please note that technical editing may introduce minor changes to the text and/or graphics, which may alter content. The journal's standard Terms & Conditions and the Ethical guidelines still apply. In no event shall the Royal Society of Chemistry be held responsible for any errors or omissions in this *Accepted Manuscript* or any consequences arising from the use of any information it contains.

ROYAL SOCIETY OF CHEMISTRY

www.rsc.org/softmatter

Graphic abstract

We theoretically and numerically demonstrate a novel soft metamaterial based on silica-coated gold core/shell-structured nanorod fluids, which shows an electrically tunable negative refraction property in visible optical region under external electric field stimuli.

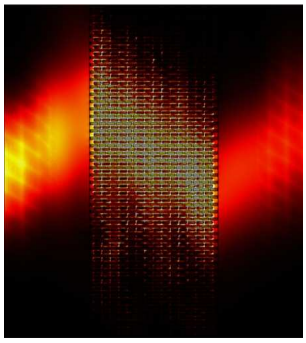

Soft Matter Accepted Manuscript

Soft Matter

RSCPublishing

ARTICLE

Electrically tunable negative refraction in core/shell-structured nanorod fluids

Cite this: DOI: 10.1039/x0xx00000x

Zhaoxian Su[a], Jianbo Yin[a,*], Yanqing Guan[a] and Xiaopeng Zhao[a]

Received 00th January 2012,
Accepted 00th January 2012

DOI: 10.1039/x0xx00000x

www.rsc.org/

We theoretically investigate an optical refraction behavior in a fluid system which contains silica-coated gold nanorods dispersed in silicone oil under an external electric field. Because of the formation of chain-like or lattice-like structure of dispersed nanorods along electric field, the fluid shows a hyperbolic equifrequency contour characteristic and, as a result, all-angle broadband optical negative refraction for transverse magnetic waves propagating can be realized. We calculate the effective permittivity tensor of the fluid and verify the analysis using finite element simulations. We also find that the negative refractive index can vary with the electric field strength and external field distribution. Under a non-uniform external field, the gradient refraction behavior can be realized.

Introduction

Metamaterials are a type of artificial materials, which have abnormal physical behaviour. Left-handed metamaterial (LHM), which has negative permittivity and permeability simultaneously, is one of the most important metamaterials.[1] The electromagnetic wave in LHM shows reverse phase and group velocities, resulting in many abnormal electromagnetic behaviors, such as negative refraction, reversed Doppler shift, reversed Cherenkov radiation, and so on.[2,3] These abnormal electromagnetic behaviors make metamaterials have potential uses in superlens imaging, highly sensitive sensor, invisible cloak, and so on.[4,5]

In the past decade, many efforts have been devoted to develop various metamaterials with negative refraction.[6-10] But most of the metamaterials are fabricated based on hard solid matter. For example, LHMs are usually fabricated by periodically arranging electric/magnetic resonator units (e.g. split ring resonator, fractal tree branches, Mie resonance clusters, etc.) on hard plastic or ceramic substrates. These hard metamaterials have advantages including good structure stability and easy top-down fabrication for large-size resonator units. However, the difficulties in the fabrication of solid metamaterials constantly increase with the decrease of unit sizes in order to be satisfied with higher frequency response. Although metamaterial-based optical invisible cloak have been fabricated by the top-down approach or other micro-nano machining equipment, the methods are often high-cost and complex. On the other hand, due to the "hard" characteristic of solid matter, the structures of solid metamaterials are difficult to be further changed or adjusted once they have been fabricated. As a result, the material's behavior can't rapidly response to the external environment change (such as different electromagnetic field frequencies and strength), that is, solid metamaterials are lack of adaptability. In addition, the flexibility of solid metamaterials is relatively lack and it will limit the processing of some special products, such as flexible "invisible cloak" that can be arbitrarily curved. Therefore, exploring new material systems and preparation methods are important to the developments and applications of metamaterials.

Different from hard matter, soft matter not only has good flexibility but also can change its structure and behavior under external stimuli. This change originates from the formation of long-range self-organized or ordered structure of molecules or particles in soft matter under external fields. Specially, the ordered structure in soft matter can be controllably adjusted through the external field strength and field distribution. Considering these characteristics, some recent researches have introduced soft matter into solid metamaterials in order to adaptively control the behaviors. For example, Zhao et al have immersed a kind of metamaterial with negative permeability in a nematic liquid crystal, realizing the adjustment of the magnetic response frequency under external field.[11] We have immersed LHMs into electrorheological fluid (ER fluid) and achieved a continuous adjustment of left-handed transmission peak frequency by external electric field.[12] In these studies, however, soft matter is only acted as additive or filler of solid metamaterials. In 2006, Zhao et al. have theoretically studied the optical negative group refraction effect in pure liquid crystal

Soft Matter Accepted Manuscript

under external fields and designed a wedge sample to observe the negative group refraction by magnetic field stimuli.[13,14] Khoo et al. have observed the change of refractive index from positive to negative at infrared frequencies in a fluid composed of silver nanoparticles dispersed in nematic liquid crystal.[15] However, the narrow working temperature region largely limits the development of liquid crystal-based metamaterials.

Recently, Urzhumov et al. have theoretically proposed a new metafluid composed of tetrahedral clusters consisting of four gold nanospheres and, by simulations, demonstrated that this metafluid possessed not only negative permeability but also negative permittivity when the cluster concentration was enough high and the electric loss was enough low.[16] However, it is relatively difficult to prepare the metafluid because it needs to not only obtain perfect nanoclusters but also ensure all clusters orientate toward a fixed direction. Huang et al have theoretically proposed a ferrofluid containing Fe_3O_4@Ag nanoparticles and numerically demonstrated a negative refraction when the nanoparticles formed chain-like structures by external magnetic fields.[17] However, the use of ferrofluid in visible optical region is still limited due to the large absorption of Fe_3O_4 or other magnetic materials as core. Furthermore, compared to an electric field that is applied only by thin-film electrodes, the magnetic field is relatively complex due to large-size of magnetic coils or poles, and this largely limits device design.

In this work, we design a novel soft metamaterial based on the fluid of silica-coated gold (Au@SiO_2) nanorods (NRs) in silicone oil and theoretically demonstrate a tunable negative refraction behavior in visible region under external electric field stimuli. Here, Au NRs are chose as core because they are easy to prepare and have low loss and strong surface plasmon resonance (SPR) in visible light region, which can induce a big negative real part and small positive imaginary part of permittivity. Coating Au NRs with low-permittivity silica shell will protect the system from dielectric breakdown and large current leakage, and simultaneously provide a good compatibility and similar refractive index with silicone oil. The elongated nanorod morphology is employed because it can enhance interparticle interaction by stronger long-axis polarization and weaken Brownian motion, and thus improve the stability of electric field-induced ordered structure.[18] Without electric fields, the Au@SiO_2 NRs are randomly distributed in the fluid. When external electric fields are applied, NRs polarize and orient to form chain-like or lattice-like ordered structure after the electrostatic energy exceeds the thermal energy and, as a result, the permittivity of fluid becomes strongly anisotropic. We simulate the achievement conditions of negative refraction of transverse magnetic (TM) light in this strongly anisotropic fluid and the dependence of refractive behavior on particle concentration, electric field strength, incident wavelength, and so on. Based on the negative refraction behavior, we also study the near-field imaging of the fluid-based superlens and its smart zoom behavior as a function of electric field strength. We finally use a non-uniform electric field to induce a gradient negative refractive index in the fluid and analyse its change with electric field distribution.

Theory

The proposed fluid is made of Au@SiO_2 NRs dispersed in silicone oil. Without electric fields, the Au@SiO_2 NRs are randomly dispersed in the fluid. So the fluid is isotropic medium, and the permittivity of the fluid can be described as:

$$\varepsilon_{\text{eff}} = \begin{pmatrix} \varepsilon_{xx} & 0 & 0 \\ 0 & \varepsilon_{yy} & 0 \\ 0 & 0 & \varepsilon_{zz} \end{pmatrix}, \text{ where } \varepsilon_{xx}=\varepsilon_{yy}=\varepsilon_{zz}.$$

When the external electric fields are applied along z axis, the long-axis of Au@SiO_2 NRs start to orientate along electric field direction due to polarization-induced interparticle attraction.[19] Meanwhile, the fluid tends to transform from an isotropic medium into an anisotropic one.[20] Thus, the permittivity of fluid also becomes anisotropic, i.e. $\varepsilon_{xx}=\varepsilon_{yy}\neq\varepsilon_{zz}$. As the electric field increases and exceeds a critical value E_c, Au@SiO_2 NRs will orientate and arrange into a gap-spanning ordered chain and even lattice structure between electrodes.[20] Especially, according to the phase transition mechanism of electro-responsive or magneto-responsive smart fluids,[21] the phase transition of nanorod fluid is of a second order transition. With the increase of applied electric field, the structure of the fluid changes gradually from isotropy to anisotropy, and as a result, the permittivity of fluid gradually changes from isotropy to anisotropy with the electric field strength. Thus, we can realize a controllable adjustment about the structure and dielectric properties of fluid through electric field.

When a beam of incident light enters into this field-induced structured fluid from free space, its refractive behavior will be influenced by the change of dielectric properties of fluid. If the light wavelength (λ) is much larger than the radius (r) of Au NRs, the length (l) of Au NRs, the thickness (d_{shell}) of silica shell, and the lattice distance (or the gap between nanorods) (d), the whole fluid system can be regarded as an effective uniaxial medium and the optical axis is along the nanorod chain or lattice orientated direction, i.e. the direction of applied electric field (z-axis direction). We can utilize the dynamic Maxwell-Garnett (M-G) theory to calculate the effective permittivity of the global fluid because M-G theory is very simple and effective for the calculation of dielectric parameters of a mixture system of inclusions immersed in a host medium. [22,23] Of course, the weakness of M-G theory is to cause inaccurate results or deviations from actual situation when the volume fraction of inclusions is very large or the geometry dimension of the inclusion particles is comparable to the wavelength of insert

Soft Matter Accepted Manuscript

 This journal is © The Royal Society of Chemistry 2013

electro-magnetic wave. However, the diameter of the inclusion particles in our proposed fluid of Au@SiO_2 NRs (r= 10 nm, l=60 nm for Au core, and d_{shell}= 5 nm for SiO_2 shell, which will be described in detail later) is much smaller than the wavelength of insert electro-magnetic wave, which is satisfied with the assumptions of M-G theory. Thus, under electric fields, the permittivity of fluid parallel to electric field (ε_{zz}) and perpendicular to electric field (ε_{xx}=ε_{yy}) can be given by following M-G equations (1) and (2):[22,23]

$$\varepsilon_{zz} = (1-\phi_g)\varepsilon_f + \phi_g\varepsilon_g \quad (1)$$

$$\varepsilon_{xx} = \varepsilon_f + \frac{\phi_g\varepsilon_f(\varepsilon_g-\varepsilon_f)}{\varepsilon_f+(1-\phi_g)(\varepsilon_g-\varepsilon_f)g_x} \quad (2)$$

Here ϕ_g is the volume fraction of Au NRs, ε_g and ε_f are relative permittivity of Au NRs and surrounding medium respectively. Because the dielectric properties of SiO_2 shell are similar to silicone oil, we can take them as a homogenous medium with the same permittivity of $\varepsilon_f = 2.13$ ($\varepsilon_f = n_f^2$ $n_f = 1.46$ is the refractive index[24]). Thus, the fluid can be regard as a simple two-phase system containing ellipsoidal inclusions (Au NRs) immersed in host medium (silicone oil). We simplify a single Au NR as a prolate ellipsoid and its long axis is along the direction of external electric field. Hence, g_x and g_z are the effective depolarization factors of an individual Au NR perpendicular to the electric field and parallel to the electric field, respectively. Depolarization factors reflect the influence of shape anisotropy of particles on dielectric properties. They satisfy a simple geometry rule of $g_z + 2g_x$=1 and g_z can be obtained by an approximate equation (3):[25]

$$g_z = \frac{e^2}{2e^3}\left(\ln\frac{1+e}{1-e} - 2e\right) \quad (3)$$

where $e = \sqrt{1-(2r/l)^2}$ is the eccentricity. The permittivity (ε_g) of Au NRs in equations (1) and (2) is derived from Drude model, i.e. $\varepsilon_g = 1 - \frac{\omega_p^2}{\omega(\omega+i\gamma_d)}$ (where $\omega_p = 1.37\times10^{16}s^{-1}$ is bulk plasmon frequency of Au and $\gamma_d = 4.08\times10^{13}s^{-1}$ is the collision frequency).[26] Thus, according to equations (1) and (2), when the volume fraction of Au is sufficient, this electric field-induced anisotropic fluid can possess ε_{xx}=ε_{yy}>0 and ε_{zz}<0, which can be called as "indefinite medium".[27]

According to Maxwell's equations, the dispersion relation for the TM light with the magnetic field component polarized in the y-axis and the electric field component located in the x-z plane propagating in such indefinite medium follows the equation (4):

$$k_x^2/\varepsilon_{zz} + k_z^2/\varepsilon_{xx} = \omega^2/c^2 \quad (4)$$

where c is the speed of light in vacuum, k_x and k_z are the wave vectors along x-axis and z-axis in such medium, respectively. Equation (4) indicates that the equifrequency contour of such medium is hyperbolic in the (k_x, k_z) plane. Thus, the time-averaged Poynting vector S in x-axis and z-axis can be written as $\boldsymbol{S}_x = \frac{k_x}{\varepsilon_{zz}}\frac{H_y^2}{2\omega\varepsilon_0}$ and $\boldsymbol{S}_z = \frac{k_z}{\varepsilon_{xx}}\frac{H_y^2}{2\omega\varepsilon_0}$, respectively.[28] The refractive angles (φ) of wave vector k and Poynting vector S are given by equation (5) and equation (6), respectively: [28]

$$f_k = \tan^{-1}(k_x/k_z) \quad (5)$$

$$\phi_s = \tan^{-1}(S_x/S_z) = \tan^{-1}[(k_x\varepsilon_{xx})/(k_z\varepsilon_{zz})] \quad (6)$$

The effective refractive index of the indefinite medium is $\eta = \sin\theta/\sin\varphi_s$, where θ is the incident angle of TM light. Because of the continuity of tangential component (k_x) of wave vector, the hyperbolic equifrequency contour, and the causality theorem, the sign of $\boldsymbol{S}_x$ will flip at the interface between air and medium when an TM light is incident from air to such indefinite medium[17,28,29] Thus, the real part of φ_s is negative (i.e. $\mathrm{Re}(\theta_s) < 0$) and a negative refraction occurs. Obviously, the effective refractive index η is negative according to η=sinθ/sinϕ_s. Therefore, we can achieve all-angle negative refraction in this electric field-induced structured nanorod fluid that has an anisotropic permittivity ($\varepsilon_{xx} = \varepsilon_{yy} > 0$, $\varepsilon_{zz} < 0$).

Based on the theory analysis above, we employ the Au@SiO_2 NRs with size parameters of r= 10 nm, l=60 nm for Au core, and d_{shell}= 5 nm for SiO_2 shell as dispersal phase. The dimension of NRs is satisfied with the assumptions of M-G theory and is easy to be prepared by wet-chemical methods.[30,31] To realize ε_{zz}<0 in this fluid (e.g. at 564 THz), the volume fraction (ϕ_g) of Au needs to be larger than 0.13 according to equation (1). We choose two typical volume fractions of ϕ_g = 0.15 and 0.19 in order to calculate expediently. Thus, the total volume fraction (ϕ) of the Au@SiO_2 NRs is 0.39 and 0.51 by $\phi_g = \frac{l}{l+2d_{shell}}\frac{r^2}{(r+d_{shell})^2}\phi = 0.38\phi$. According to reported phase diagrams of particle suspension system under electric fields,[32,33] the nanorods orientate along electric fields and tend to arrange into body centered tetragonal (BCT) lattice at ϕ =0.39 as showed in Fig.1 (a) and (c), while the nanorods tend to form hexagonal lattice at ϕ=0.51 as showed in Fig.1 (b) and (d). Fig. 2 shows the calculated permittivities of the fluid at the ϕ=0.39 and ϕ=0.51 according to equations (1) and (2), respectively. It can be found that, in a broad frequency region, the real part of ε_{zz} is negative and the real part of ε_{xx} (or ε_{yy}) is positive. Therefore, it is possible to achieve all-angle negative refraction in this electric field-induced structured nanorod fluid.

Soft Matter Accepted Manuscript

To confirm these, we numerically simulate our design in the following section.

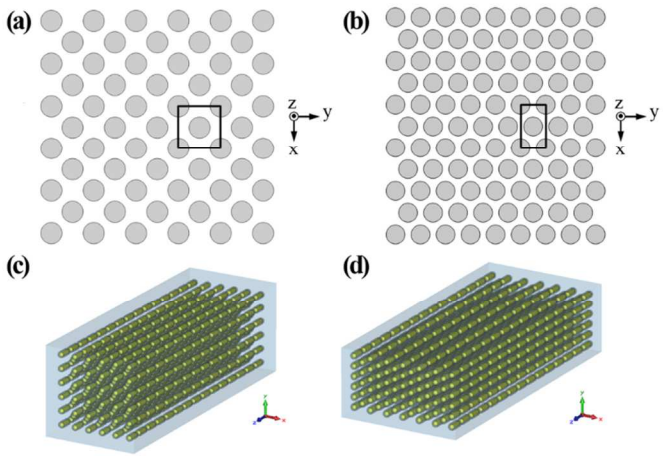

Fig. 1 The schematic illustration of cross-section of the lattice perpendicular to the electric field for the fluid of Au@SiO_2 NRs at $\phi = 0.39$ (a) and $\phi = 0.51$ (b). The schematics of the lattice of the chains formed by Au@SiO_2 NRs at $\phi = 0.39$ (c) and $\phi = 0.51$ (d). The rectangular unit cells are adopted in the finite-element simulations for $\phi = 0.39$ and $\phi = 0.51$ respectively.

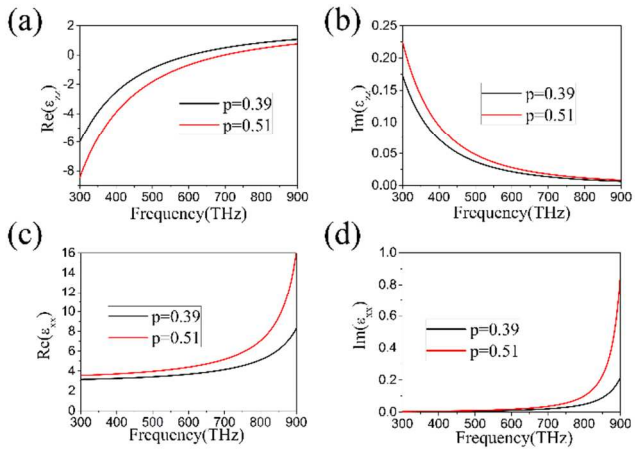

Fig. 2 (a) Real part and (b) image part of the effective permittivity parallel to the electric field for the fluid of Au@SiO_2 NRs in silicone oil; (c) Real part and (d) image part of the effective permittivity perpendicular to the electric field for the fluid of Au@SiO_2 NRs in silicone oil. (black line: $\phi = 0.39$; red line: $\phi = 0.51$).

Numerical simulations and discussions

Electric field-induced formation of negative refractive index

The software COMSOL Multiphysics 4.3 is used to numerically demonstrate our design based on the finite element method (FEM). Firstly, in the simulation, two kinds of fluids of Au@SiO_2 NRs in silicone oil with particle volume fraction ϕ =0.39 and $\phi = 0.51$ are employed based on the theory analysis above. According to reported phase diagrams, under electric fields the NRs orientate and tend to arrange into BCT lattice as showed in Fig.1 (a) and (c) at ϕ=0.39, while the NRs tend to form hexagonal structure as showed in Fig.1 (b) and (d) at ϕ =0.51.[33] Secondly, we regard the silica shell of NRs and surrounding silicone oil as a homogeneous medium due to their similar permittivity and optical property. The size of NRs is r=10 nm and l=60 nm in simulation, which is much smaller than the incident light wavelength. This is in accordance with the assumptions of theory above. Thirdly, we set the sample thickness (i.e. the gap between electrodes) as 1050 nm that is larger than wavelength. Both sides of the sample are air. We ignore the electrode's thickness and surface or anchoring effects from electrodes for nanorod orientation. The nanorod orientation is only controllably adjusted by external electric fields. Finally, we take a transverse magnetic (TM) Gaussian beam (magnetic field component is polarized along the y–axis, electric field component located in the x-z plane) with a width of 1000 nm as incident light and the incident angle (θ) is 30°. The distance between light source and sample is 700 nm.

At particle volume fraction ϕ =0.39, the electric field-induced chains tend to form BCT fashion as shown in Fig. 1(a) and (c).[33] We set the lattice constant as d=60 nm ($\phi = (2\pi r^2)/d^2$) and employ $n_x \times n_y \times n_z$ =45×1×15 unit cells in the simulation box. The number of NRs is 1350. The periodic boundary condition is used along x-axis and y-axis. Fig. 3(a) shows the cross-sectional view of the power flow in the x-z plane. It clearly shows a negative refraction. Fig. 3(b) shows the simulation by replacing the fluid system with a homogenous slab whose effective permittivity is calculated from equation (1) and equation (2). It can be found that the negative refraction is in accordance with the result in Fig. 3(a) so that it is reasonable to use the dynamical Maxwell-Garnett theory to analyse the system. The realization of negative refraction in the fluid of Au@SiO_2 NRs can be attributed to the fact that the value of ε_{zz} changing from positive to negative under electric fields.

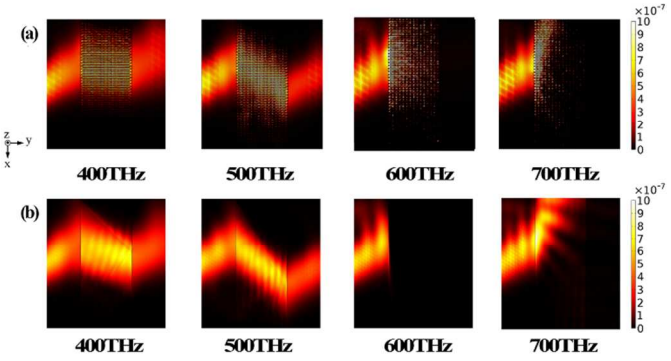

Fig. 3 Simulation results for the fluid of Au@SiO_2 NRs in silicone oil at Φ=0.39 under electric fields: (a) the time average power flow at incident wave frequency

Soft Matter Accepted Manuscript

This journal is © The Royal Society of Chemistry 2013

400 THz, 500 THz, 600 THz, and 700 THz respectively. In the simulation, the chains, constituted by end-to-end Au@SiO_2 NRs, are arranged in BCT structure; (b) the simulation at corresponding frequency based on the effective medium approximation which agrees with (a).

At particle volume fraction ϕ =0.51, the electric field-induced chains tend to form hexagonal fashion as shown in Fig. 1(b) and (d).[30] We set the lattice constant as d=40 nm ($\phi=(2\pi r^2)/\sqrt{3}d^2$) due to higher particle concentration and employ $n_x \times n_y \times n_z$ =40×1×15 unit cells in the simulation box. The number of NRs is 1200. The periodic boundary condition is also used along x-axis and y-axis. Fig. 4 demonstrates the negative refraction still appears in the system with hexagonal structure because the fluid system still can be regard as an effect uniaxial medium in this situation. The simulation result replacing the fluid structure with a homogenous slab in Fig. 4(b) is still agreement with that in Fig. 4(a). However, it should be pointed out that, because the refractive index is determined by the concentration of Au core and the frequency of incident light, the value of refractive index of the Poynting vector in Fig. 4 is different from that in Fig. 3, because the volume fraction of Au core is lager for $\phi = 0.51$.

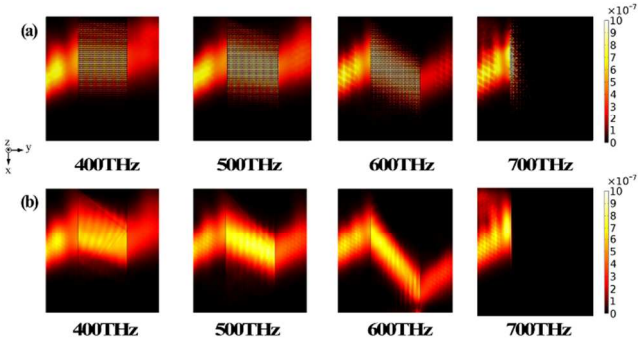

Fig. 4 Simulation results for the fluid of Au@SiO_2 NRs in silicone oil at Φ=0.51 under electric fields: (a) the time average power flow at incident wave frequency 400 THz, 500 THz, 600 THz, and 700 THz respectively. In the simulation, the chains, constituted by end-to-end NRs, are arranged in hexagonal structure; (b) the simulation at corresponding frequency based on the effective medium approximation which agrees with (a).

Furthermore, from Fig. 3 we can find the refractive angle of the time average power flow becomes lager as the incident light frequency increases from 400 THz to 600 THz. The variety of the refractive angle is induced by the change of the permittivity of the system at different incident wave frequencies. Because the real part of the permittivity of Au follows the Drude mode, ε_{zz} tends to gradually become zero with the increase of the incident wave frequency at the certain concentration of Au NRs. At 700 THz, Fig. 3 shows there is a strong absorption. According to above calculation, the real part of ε_{zz} is nearly zero at the incident wave frequency 700 THz when $\phi = 0.51$. This frequency corresponds to the so-called longitudinal SPR.[34] For a Drude metal with $\varepsilon_g = 1 - f_p^2/f^2$ and f_p the plasmon frequency, one has the so-called longitudinal SPR frequency $f_l = f_p(1 + (\phi_g^{-1} - 1)\varepsilon_f)^{-1/2}$. Thus, f_l is very sensitive to the volume fraction ϕ_g and permittivity ε_f of the surrounding medium. The smaller the ε_f, the higher the longitudinal SPR frequency f_l. Obvious, decreasing the volume fraction of the Au NRs results in a redshift of the longitudinal SPR frequency. Therefore, in Fig. 4, the strong absorption corresponding to the so-called longitudinal appears at the incident wave frequency 600 THz due to reducing of the concentration of Au NRs. Because ε_{zz} is positive at 700 THz when $\phi = 0.39$, the refractive angle is positive at 700 THz, which is presented in Fig. 3. We can change this frequency by adjusting the lattice constant of the system, i.e., the volume fraction of Au NRs.

On the other hand, the permittivity match between the shell of core/shell-structured NRs and the surrounding medium is important to negative refraction behavior. Fig. 5 compares the negative refraction behaviors of the nanorod fluid with different permittivity match between the shell of NRs and the surrounding medium. For example, ε_{shell}=~2.13 for Au@SiO_2 NRs, ε_{shell}=~2.40 for Au@Al_2O_3 NRs, and ε_{shell}=~6.50 for Au@TiO_2 NRs. It can be found that the transmission level declines as the permittivity difference between the shell of NRs and the surrounding medium becomes large. When ε_{shell}=~6.50 for Au@TiO_2 NRs in silicone oil, a longitudinal SPR occurs in the fluid which leads to a strong absorption and the negative refraction behavior disappears. Therefore, we suggest using silica (ε_{shell}=~2.13) as coating shell to not only provide an effectively insulating effect for Au core but also provide a good permittivity match between the shell of NRs and the surrounding medium (ε_f=~2.13 for silicone oil, which depends on molecular structure) in order to obtain the optimal negative refraction effect.

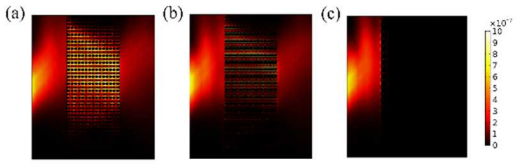

Fig. 5 The time averaged power flow of the fluid of NRs with different permittivity match between the shell of NRs and the surrounding medium at Φ=0.51 under electric fields: (a) Au@SiO_2 NRs with ε_{shell}=~2.13; (b) Au@Al_2O_3 NRs with ε_{shell}=~2.40; (c) Au@TiO_2 NRs with ε_{shell}=~6.50. The surrounding medium is silicone oil with ε_f=~2.13 that depends on molecular structure. (The frequency of incident light is 500THz and incident angle is 30°)

The shape anisotropy or aspect ratio of NRs also has an effect on negative refraction behaviour. Fig. 6 shows the simulate results of the negative refraction behavior as a function of the aspect ratio of

Soft Matter Accepted Manuscript

NRs at the same Au volume fraction. It is found that the negative refraction angle of the time average power flow becomes lager as the increase of shape anisotropy or aspect ratio of NRs. This can be ascribed to that fact that the increase of the shape anisotropy or aspect ratio enhances the permittivity anisotropy of the fluid. Therefore, to enhance negative refraction behavior, we had best use NRs with large aspect ratio as disperse phase.

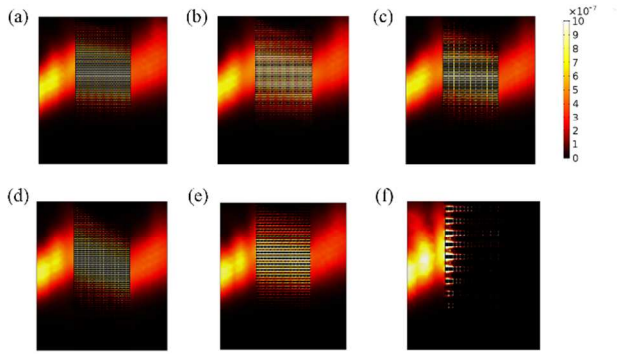

Fig. 6 Time average power flow of the fluid of $Au@SiO_2$ NRs with various aspect ratio at Φ=0.51 under electric fields: (a) r=10 nm, l=45 nm; (b) r=10 nm, l=60 nm; (c) r=10 nm, l=90 nm; (d) r=7.5 nm, l=60 nm; (e) r=15 nm, l=60 nm (f) r=30 nm, l=60nm. (The frequency of incident light is 500THz and incident angle is 30°)

In addition, it should point out that the negative refraction in the nanorod fluid is tolerant to the deviation of perfect lattice. Compared to the negative refraction effect in fluid with perfect lattice (Fig. 7(a)), the negative refraction effect in Fig. 7(b) is still strong even if there are some defects (such as small-size nanorod aggregations) whose size is significantly smaller than the incident light wavelength. This can be attributed to the fact that the structured fluid containing small-size defects is still regarded as the effective media approximation. If there appear some large-size defects (such as large-size nanorod aggregations) in the lattice, however, the optical transmission and negative refraction behavior are compressed (see Fig. 7(c)) because the large-size defects can act as scattering centers and the effective media approximation is not valid. Therefore, to enhance negative refraction behavior, we should make electric field–induced nanorod arrangement as perfect or effective as possible and try to avoid large-size nanorod aggregations. One effective way to avoid nanorod aggregations is to increase colloid repulsive force of NRs by surface charge in preparation.

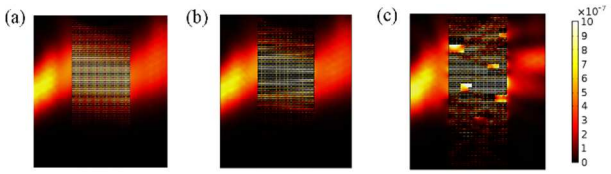

Fig. 7 The time averaged power flow of the fluid of $Au@SiO_2$ NRs in silicone oil at Φ=0.51 under electric fields: (a) NRs orientate and arrange into perfect lattices; (b) NRs orientate and arrange into lattices containing defects (small-size nanorod aggregations) whose size is smaller than incident light wavelength; (c) NRs orientate and arrange into lattices containing defects (large-size nanorod aggregations) whose size is larger than incident light wavelength. (The frequency of incident light is 500THz and incident angle is 30°)

Electric field strength dependence of negative refractive index and electrically tunable image

In this section, we analyze the dependence of the refractive index on electric field strength in detail. Without electric fields, the particles are randomly distributed and the fluid is isotropic, whose permittivity $(\varepsilon_{xx} = \varepsilon_{yy} = \varepsilon_{zz} = \varepsilon_{eff})$ can be approximately calculated by the Looyenga formula as shown in equation (7) [35]:

$$\varepsilon_{\text{eff}} = \left(\varepsilon_{\text{f}}^{1/3} + \phi_{\text{g}}\left(\varepsilon_{\text{f}}^{1/3} - \varepsilon_{\text{g}}^{1/3}\right)\right)^3 \qquad (7)$$

When the external electric fields are applied along z-axis, the long-axis of $Au@SiO_2$ NRs starts to orientate along electric field direction. Meanwhile, the fluid tends to transform from isotropic medium into anisotropic medium. As the external electric field strength increases, NRs form chains along the direction of the field, which cause the system to be more anisotropic. It has been demonstrated that the permittivity of particle fluid is linearly dependent on electric field strength when the particles start to orientate and align [36]. When the electric field exceeds a critical value (E_c), all particles have form gap-spanning chain structure between electrodes and, as a result, the whole system can be regarded as an effect uniaxial medium whose permittivity become constant. Thus, the relation of the fluid permittivity parallel to electric field ($\boldsymbol{\varepsilon_{zz}}$) can be expressed by equation (8) and the fluid permittivity perpendicular to electric field ($\boldsymbol{\varepsilon_{xx}}$, $\boldsymbol{\varepsilon_{yy}}$) can be expressed by equation (9):

$$\varepsilon_{zz} = \begin{cases} \varepsilon_{\text{eff}} = \left(\varepsilon_{\text{f}}^{1/3} + \phi_{\text{g}}\left(\varepsilon_{\text{f}}^{1/3} - \varepsilon_{\text{g}}^{1/3}\right)\right)^3, \ E = 0 \\ \varepsilon_{eff} + k_1 E, \ 0 < E < E_{\text{c}} \\ \varepsilon_{eff} + k_1 E_{\text{c}}, \ E \gg E_{\text{c}} \end{cases} \qquad (8)$$

$$\varepsilon_{\text{xx,yy}} = \begin{cases} \varepsilon_{\text{eff}} = \left(\varepsilon_{\text{f}}^{1/3} + \phi_{\text{g}}\left(\varepsilon_{\text{f}}^{1/3} - \varepsilon_{\text{g}}^{1/3}\right)\right)^3, \ E = 0 \\ \varepsilon_{\text{eff}} + k_2 E, \ 0 < E < E_{\text{c}} \\ \varepsilon_{\text{eff}} + k_2 E_{\text{c}}, \ E \gg E_{\text{c}} \end{cases} \qquad (9)$$

In these equations, k_1 and k_2 are constant. In experiment realization, the critical field strength E_c is the key to the formation of chains of NRs. Here, E_c can be estimated by the

Soft Matter Accepted Manuscript

 This journal is © The Royal Society of Chemistry 2013

ratio of electric field energy to thermal energy as shown in equation (10):[37]

$$\frac{1}{3}\pi lr^2\varepsilon_0\varepsilon_f \mathrm{Re}(K_L)E_c^2 \gg \frac{3}{2}k_B T \qquad (10)$$

where K_L is the Clausius-Mossotti factor given by $K_L = (\varepsilon_g - \varepsilon_f)/[(\varepsilon_g - \varepsilon_f)g_z + \varepsilon_f]$. Here, $\varepsilon_g = 1 + i\sigma/\omega$ represents the permittivity of Au NRs at applied low-frequency AC electric field with angle frequency ω, σ is the conductivity of gold. The reason we choose AC electric field is that the dielectrophoresis of Au@SiO_2 NRs will be decreased and thus the chains are more stable. So the critical field strength can be estimated as by equation (11):

$$\boldsymbol{E}_c \approx \sqrt{\frac{9k_B T}{2\pi lr^2\varepsilon_0\varepsilon_f \mathrm{Re}(K_L)}} \qquad (11)$$

At $T = 300$ K and $\omega = 50$ kHz, the critical field value is about 2.39×10^6 V/m. Thus, we need to apply at least a voltage of 2.51 V on a 1050 nm-thick fluid system in the reality experiment. At the same time, the voltage is independent of particle volume fraction. So when the electric field strength reaches 2.39×10^6 V/m, almost all Au@SiO_2 NRs form chains. Fig. 8 gives the calculated value of permittivity of fluid at the incident wave frequency of 564 THz as a function of electric field strength according to equations (8) and (9). It can be found that the real part of permittivity of the fluid changes from isotropic to anisotropic when the electric field strength is lower than 2.39×10^6 V/m and then becomes constant when the electric field strength is higher than 2.39×10^6 V/m. At the same time, the image part of the permittivity parallel and perpendicular to z-axis decreases with the increase of anisotropic ordered structure.

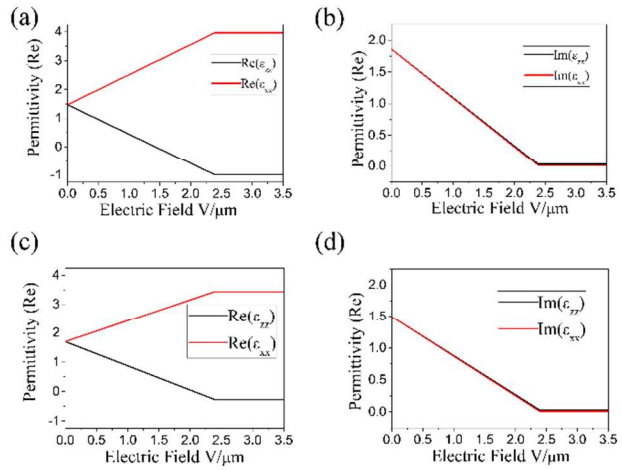

Fig. 8 The dependence of permittivity of the fluid of Au@SiO_2 NRs in silicone oil on applied electric field strength at the incident wave frequency of 564 THz. (a) Real and (b) imaginary part of the permittivity at $\phi = 0.51$. The permittivity of the system is changing from isotropic ($\varepsilon_{\mathrm{eff}} = 1.47 + 1.86i$) to anisotropic ($\varepsilon_{\mathrm{xx}} = \varepsilon_{\mathrm{yy}} = 3.96 + 0.01i$, $\varepsilon_{zz} = -0.99 + 0.03i$) in the electric field region between 0 and E_c; (c) Real and (d) imaginary part of the permittivity at $\phi = 0.39$. The permittivity of the system is changing from isotropic ($\varepsilon_{\mathrm{eff}} = 1.70 + 1.49i$) to anisotropic ($\varepsilon_{\mathrm{xx}} = \varepsilon_{\mathrm{yy}} = 3.43 + 0.01i$, $\varepsilon_{\mathrm{zz}} = -0.27 + 0.03i$) in the electric field region between 0 and E_c

Fig. 9 shows the time average power flow simulation at the incident optical frequency of 564 THz and ϕ=0.51 as a function of electric field strength. It can be found that the loss of incident wave gradually decreases and the negative refraction is realized at sufficient high field strength. This can be attributed to that the structure of the system will transform from isotropic fluid to a uniaxial medium with the increasing of electric field strength, the loss of incident wave will decline, according to the imaginary part of the permittivity decreasing in Fig. 8.

Because of the anisotropic permittivity of the system under external electric field, the fluid is a kind of indefinite medium.[31] Image of uniaxial indefinite material has been demonstrated in the theory and experiment.[34] Therefore, we also numerically demonstrate that such a fluid system can be used for imaging. Fig. 10 shows the time-averaged power flow in the 3D finite-element simulation for the incident wave of 564 THz in the fluid with $\phi = 0.51$. In the FEM simulation depicted in Fig. 8, the point source of light located 200 nm in front of a 1050 nm-thick fluid system. It can be found that a clearly elongated focus point emerges when the wave traverse the fluid. Because the effective refraction index of the indefinite material is angle-dependent, there is an aberration of the imaging [38].

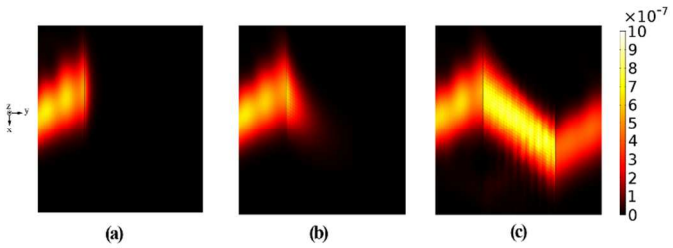

Fig. 9 The time average power flow simulation based on the effective medium approximation for the fluid of Au@SiO_2 NRs in silicone oil at $\phi = 0.51$ according to the permittivity calculated in Fig. (5) at the incident wave frequency of 564THz under different external electric field strength of (a) $E = 0$, (b) $E = 2\times10^6$V/m, and (c) $E = 2.39\times10^6$V/m

Soft Matter Accepted Manuscript

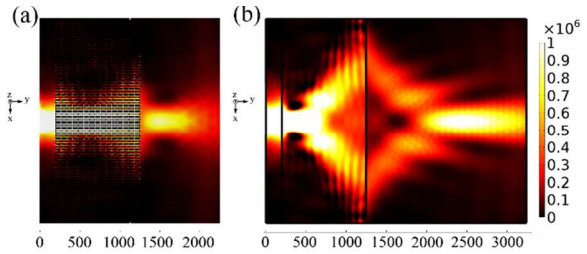

Fig. 10 The time-averaged power flow imaging in the 3D finite-element simulation for the incident wave of 564THz in the fluid of Au@SiO_2 NRs in silicone oil at ϕ=0.51. (a) 3D finite-element simulation and (b) effective medium approximation simulation.

The deviation of the focus distance in Fig. 10(a) and (b) results from the interaction of the internal units in the fluid system. The image is realized by the hyperbolic equifrequency surface.[31] We can change the permittivity of the system by adjusting the external electric field strength to realize the subwavelength and magnified imaging.[39,40] When the permittivity of the fluid system changes with external electric field strength, the focus of fluid lens system will change with the electric field strength. This situation is plotted in Fig. 11, in which the fluid system is replaced by a homogenous medium. As shown in Fig. 11, the distance between the focus and the fluid lens becomes small as the electric field strength increases. Thus, the fluid system can be used as a smart fluid lens whose focus distance can be adjusted via external field strength.

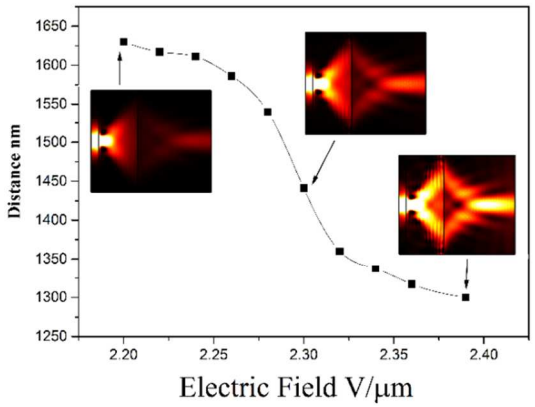

Fig. 11 The dependence of the distance between the focus point and the fluid lens on electric field strength for the incident wave of 564 THz in the fluid of Au@SiO_2 NRs in silicone oil at ϕ=0.51.

Electric field distribution dependence of negative refractive index and gradient negative refractive index

Besides the electric field strength, the distribution of electric field will influence the structure of NRs or the lattice parameter in gap-spanning chain structure. For example, when a non-uniform radial electric field is applied, the Au NRs will form radial chain-like structure and, as a result, the lattice constant d or distance between chains will be continuously changed. Thus the concentration of the Au NRs will not be uniform in this situation and it should be a function of coordinate. From equations (1) and (2), we can find that the permittivity of the system is determined by the volume fraction of Au NRs when other conditions are constant. The local concentration of Au NRs will gradually decreases along z-axis when a non-uniform radial electric field is applied, which causes ε_{zz} gradually to decrease along z-axis. Therefore, the refractive angle of the time average power flow will increase along z-axis and the graded negative refraction can be obtained.

In the simulation of the fluid system under the non-uniform radial electric field, the number of unit cells along x-axis decreases from 40 to 28, indicating that the volume fraction of NRs decreases from 0.51 to 0.36. The number of unit cells along z-axis remain 15. The degree of concentration decline is proportional to the non-uniformity of the electric field. Replacing the system by a homogenous slab, we firstly simulated the refractive behavior under different non-uniform radial electric fields based on the effective medium approximation as shown in Fig. 12. It shows the refractive deflection effect increases with the increase of the non-uniformity of electric field. Fig. 13 compares the negative refraction results by finite element simulations under a uniform field and a non-uniform electric field. It is found that the negative refraction of time average power flow is graded when the lattice constant d is gradually increased due to the change of external electric field distribution due to the gradient permittivity.

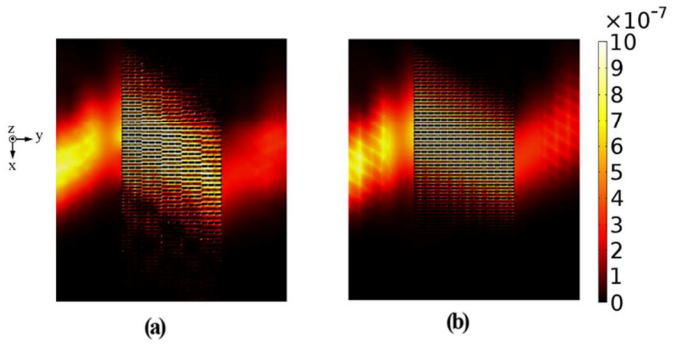

Fig. 12 The time-averaged power flow simulation based on the effective medium approximation in the fluid of Au@SiO_2 NRs in silicone oil under a uniform field (a) and non-uniform electric field (b-d). (b): particle concentration ϕ change from 0.51 to 0.47; (c): particle concentration ϕ change from 0.51 to 0.45; (d): particle concentration ϕ changes from 0.51 to 0.42.

Soft Matter Accepted Manuscript

This journal is © The Royal Society of Chemistry 2013

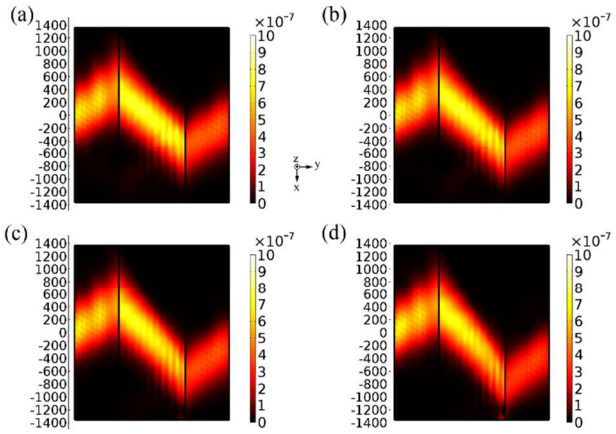

Fig. 13 The cross-sectional view of finite element simulations: (a) The negative refraction of time average power flow is graded when lattice constant *d* is gradually increase due to the change of external electric field distribution. (b) The negative refraction of time average power flow at uniform electric field. The electric field-induced chains displaced in hexagonal structure.

Conclusions

In summary, we have designed a fluid system containing Au@SiO_2 NRs in silicone oil, which can realize all-angle broadband negative refraction at optical frequencies under external electric fields because of the formation of chain-like or lattice-like structure of dispersed NRs along electric fields. We calculate the effective permittivity tensor of the fluid and verify that, in a broad spectra region, the real part of $\boldsymbol{\varepsilon_{zz}}$ is negative and the real part of $\boldsymbol{\varepsilon_{xx}}$ (or $\boldsymbol{\varepsilon_{yy}}$) is positive. Thus, we can realize all-angle negative refraction in the fluid system because of the hyperbolic equifrequency surface and the boundary condition for electromagnetic waves at the interface between a uniaxial medium and an isotropic medium. The refractive index can vary with the electric field strength and external field distribution because that the effective permittivity tensor of the fluid can change with electric fields. Based on this point, we further demonstrate a near-field imaging in the fluid-based superlens under uniform electric field and a negative refractive index gradient under non-uniform electric field. This novel fluid with electrically tunable negative refraction not only proposes a new strategy to fabricate soft metamaterials but also provides a foundation for the future development of smart metamaterial devices, such as adaptive fluid-based super lens, flexible "cloak",[41] and so on.

Acknowledgements

This work is supported by the Program for New Century Excellent Talents in University of China, National Natural Science Foundation of China (no. 51272214), and NPU Foundation for Fundamental Research (no. JC20120247).

Notes and references

[a]*smart Materials Laboratory, Department of Applied Physics, Northwestern Polytechnical University, Xi'an 710129, P. R. China.*
E-mail: jbyin@nwpu.edu.cn

1 V. G. Veselago, Sov. *Physics-Uspekhi*, 1968,**10**, 509.
2 N. Seddon and T. Bearpark, *Science*, 2003, **302**, 1537-1540.
3 A. Grbic and G. V. Eleftheriades, *Journal of Applied Physics*, 2002, **92**, 5930-5935.
4 J. B. Pendry, *Phys. Rev. Lett.*, 2000, **85**, 3966.
5 J. B. Pendry, D. Schurig and D. R. Smith, *Science*, 2006, **312**,1780.
6 R. A. Shelby, D. R. Smith and S. Schultz, *Science*, 2001, **292**, 77-79.
7 J. Yao, Z. Liu, Y. Liu, Y. Wang, C. Sun, G. Bartal, A. M. Stacy, X. Zhang, *Science*, 2008, **321**, 930-930.
8 H. Shin and S. Fan, *Phys. Rev. Lett.*, 2006, **96**, 073907.
9 J. B. Pendry, *Science*, 2004, **306**, 1353-1355.
10 A. Pimenov, A. Loidl, P. Przyslupski P and B. Dabrowski, *Phys. Rev. Lett.*, 2005, **95**, 247009.
11 Q. Zhao, L. Kang, B. Du, J. Zhou and H. Tang, *Appl. Phys. Lett.*, 2007, **90**, 011112.
12 Y. Huang, X. Zhao, L. Wang and C. Luo, *Progress in Natural Science*, 2008, **18**, 907-911.
13 Q. Zhao, L. Kang, B. Li, Zhou and H. Tang, *Appl. Phys. Lett.*, 2006, **89**, 221918.
14 L. Kang, Q. Zhao, B. Li, J. Zhou and H. Zhu, *Appl. Phys. Lett.*,2007, **90**, 181931.
15 D. H. Werner, D. H. Kwon, I. C. Khoo, A. V. Kildishev and V. M. Shalaev, *Opt. Express*, 2007, **15**, 3342.
16 Y. A. Urzhumov, G. Shvets, J. Fan, F. Capasso, D. Brandl and P. Nordlander, *Opt. Express*, 2007, **15**, 14129.
17 Y. Gao, J. P. Huang, Y. M. Liu, L. Gao, K. W.Yu and X. Zhang, *Phys. Rev. Lett.*, 2010, **104**, 034501.
18 J. B. Yin, X. P. Zhao, X. Xia, L. Q. Xiang and Y. P. Qiao, *Polymer*, 2008, **49**, 4413
19 W. Ahmed, E. S. Kooij, A. van Silfhout and B. Poelsema, *Nano letters*, 2009, **9**, 3786.
20 W. Wen, X. Huang and P. Sheng, *Soft Matter*, 2008, **4**, 200.
21 R. T, Physical Review E, 1993, **47**, 423.
22 A. Shivola. *Electromagnetic mixing formulas and applications*, IEE, M[J]. Faraday House, Stevenage, UK, 1999.
23 H. Ma, W. Wen,W. Y. Tam and P. Sheng, *Advances in Physics*, 2003, **52**, 343.
24 S. V. Mutilin and T. Khasanov, *Opt. Spectrosc*, 2008, **105**, 461–465.
25 L. D. Landau, E. M. Lifshitz and L. P. Pitaevskii, *Electro-dynamics of Continuous Media*, Pergamon, New York, 1984.
26 M. A. Ordal, L. L. Long, R. J. Bell, S. E. Bell, R. R. Bell, R. W. Alexander and C. A. Ward, *Appl. Opt.*, 1983, **22**, 1099.
27 D. R. Smith and D. Schurig D, *Phys. Rev. Lett.*, 2003, **90**, 077405.
28 Y. Liu, G. Bartal and X. Zhang, *Optics express*, 2008, **16**, 15439.
29 P. A. Belov, *Microw. Opt. Technol. Lett.*, 2003, **37**, 259.
30 B. Nikoobakht and M. A. El-Sayed, *Chem. Mater.*, 2003, **15**, 195.
31 I. Gorelikov and N. Matsuura, *Nano letters*, 2008, **8**, 369.
32 A. P. Hynninen and M. Dijkstra, *Phys. Rev. Lett.*, 2005, **94**, 138303.
33 U. Dassanayake, S. Fraden and A. van Blaaderen, *The Journal of Chemical Physics*, 2000, **112**, 3851.
34 W. T. Lu and S. Sridhar, *Phys. Rev. B*, 2008, 77, 233101.
35 H. Looyenga, *Physica*, 1965, **31**, 401.
36 W. Wen, S. Men and K. Lu, *Phys. Rev. E*, 1997, **55**, 3015.

Soft Matter Accepted Manuscript

37 J. E. Kim and C. S. Han, *Nanotechnology*, 2005, **16**, 2245.
38 T. Dumelow, J. A. P. da Costa and V. N. Freire, *Phys. Rev. B*, 2005, **72**, 235115.
39 G. Shvets, S. Trendafilov, J. B. Pendry, and A. Sarychev, *Phys. Rev. Lett.,* 2007, **99**, 053909.
40 P. Ikonen, C. Simovski, S. Tretyakov, P. Belov, and Y. Hao, *Appl. Phys. Lett.*, 2007, **91**, 104102 .
41 A. B. Golovin and O. D. Lavrentovich, *Appl. Phys. Lett.*, 2009, **95**, 254104.

Soft Matter Accepted Manuscript

 This journal is © The Royal Society of Chemistry 2013